J|A|C|S
ARTICLES

Published on Web 04/14/2009

Hydrophobically Self-Assembled Nanoparticles as Molecular Receptors in Water

Salvador Tomas*,† and Lilia Milanesi‡

School of Biological and Chemical Sciences and School of Crystallography, Birkbeck, University of London, Malet Street, London WC1E 7HX, U.K.

Received January 23, 2009; E-mail: s.tomas@bbk.ac.uk

Abstract: Biomolecular and artificial receptors are typically designed to exploit the hydrophobic effect in order to enhance the stability of receptor−ligand complexes in water. For example, artificial receptors are often built around hydrophobic cavities. These receptors exploit the hydrophobic effect toward ligand recognition, but the structure of the binding site requires a rigid framework to overcome the hydrophobic effect-driven tendency to collapse. Here we present an artificial receptor that exploits the hydrophobic effect to define its structure in water. The receptor is based on amphiphilic building blocks that assemble into micelle-like aggregates of a very high stability, attributed to the unusual shape of the amphiphile: a relatively rigid molecule composed of a large hydrophobic segment, based on the cholesterol molecule, and a very large headgroup build around a Zn-metalloporphyrin moiety. The assemblies, persistent down to the nanomolar range, are better described as self-assembled nanoparticles. Within the nanoparticle−water interface, Zn-metalloporphyrin moieties form multiple binding sites that specifically bind ligands bearing basic nitrogen atoms. The nanoparticles show enhanced binding affinity relative to a model receptor that does not self-assemble. Structurally related ligands show a correlation between the enhancement of binding and the octanol/water partition coefficient, log *P*, suggesting that the desolvation of binding sites is the main driving force for the enhancement of binding affinity at the nanoparticle−water interface. In addition, the highest affinity observed for the ditopic ligands relative to the monotopic ligands is evidence of a multivalent effect operating within this type of receptors. The nanoparticle readily deassembles upon addition of water-miscible organic solvents, such as methanol, or in the presence of detergents. This approach toward self-assembled receptors can be easily adapted to the development of differential receptors by the simple expedient of mixing slightly different amphiphiles (i.e., different metals in the porphyrin ring for the amphiphiles described here) in variable proportions.

Introduction

Biomolecules are regulated by finely tuned molecular recognition events that result in highly organized biological systems. The use of simplified artificial molecules that display molecular recognition capabilities (i.e., that self-assemble or that form complexes with other molecules) allows us to study the precise mechanism of molecular recognition processes.[1] In turn, we use this knowledge to (i) understand how biological systems are organized at the molecular level[2] and (ii) develop artificial systems of increasing complexity for technological applications.[3,4] Since biomolecules work mainly in aqueous media, the development of artificial systems that work in water is especially interesting because it opens the possibility of developing tools to directly manipulate biosystems at the molecular level.[5] In water, molecular recognition events are dominated by the strong competition between the solvent and the hydrophobic effect. This makes it more difficult to develop artificial systems in water compared to less competitive solvents.[6] Nonetheless, recently there has been a steady increase of artificial systems designed to work in aqueous solution, from molecules that self-assemble in long-range structures (i.e., hydrogels,[7] polymersomes,[8] and fibers[9]) to discrete molecular-sized assemblies (i.e., molecular receptors).[6,10,11] In most cases the hydrophobic effect features prominently as the driving force behind the association processes, as it does in many biomolecular recognition events. However, we have not yet learned to fully exploit it. For example, when designing a molecular receptor in water, a widespread strategy involves building the receptor around hydrophobic cavities.[6,10] But these receptors typically require a rigid framework to overcome the hydrophobic effect-driven tendency of the binding site to collapse. In other words, while

† School of Biological and Chemical Sciences.
‡ School of Crystallography.

(1) Cockroft, S. L.; Hunter, C. A. *Chem. Soc. Rev.* **2007**, *36*, 172–188.
(2) Hunter, C. A.; Tomas, S. *Chem. Biol.* **2003**, *10*, 1023–1032.
(3) Balzani, V.; Credi, A.; Raymo, F. M.; Stoddart, J. F. *Angew. Chem., Int. Ed.* **2000**, *39*, 3349–3391.
(4) Kinbara, K.; Aida, T. *Chem. Rev.* **2005**, *105*, 1377–1400.
(5) Peppas, N. A.; Hilt, J. Z.; Khademhosseini, A.; Langer, R. *Adv. Mater.* **2006**, *18*, 1345–1360.
(6) Oshovsky, G. V.; Reinhoudt, D. N.; Verboom, W. *Angew. Chem., Int. Ed.* **2007**, *46*, 2366–2393.
(7) Deng, W.; Yamaguchi, H.; Takashima, Y.; Harada, A. *Angew. Chem., Int. Ed.* **2007**, *46*, 5144–5147.
(8) Discher, B. M.; Won, Y. Y.; Ege, D. S.; Lee, J. C. M.; Bates, F. S.; Discher, D. E.; Hammer, D. A. *Science* **1999**, *284*, 1143–1146.
(9) Ryu, J. H.; Hong, D. J.; Lee, M. *Chem. Commun.* **2008**, 1043–1054.
(10) Biros, S. M.; Rebek, J. *Chem. Soc. Rev.* **2007**, *36*, 93–104.
(11) Best, M. D.; Tobey, S. L.; Anslyn, E. V. *Coord. Chem. Rev.* **2003**, *240*, 3–15.

10.1021/ja900561j CCC: $40.75

the hydrophobic effect is exploited to enhance ligand binding, part of the effort is used in fighting against it through techniques of covalent chemistry. By contrast, biomolecules typically exploit the collapse of hydrophobic moieties to help define their structure (i.e., protein folding).[12] Clearly, with our current knowledge it is not possible to predict the three-dimensional structure resulting from the collapse of an artificial oligomeric structure in water.[13,14] However, it is possible to predict to some extent the overall structures of assemblies derived from the hydrophobic-driven collapse of amphiphilic molecules. In particular, amphiphiles will assemble into a roughly spherical micelle with a size comparable to that of a small protein, provided that the geometry of the amphiphile is the appropriate one.[15,16] Micelles are not, however, regarded as molecular receptors due to their lack of specificity and low stability (typical critical micellar concentrations, CMC, are on the order of millimolar, meaning that below this concentration the potential receptor simply does not exist).[17] In this work we introduce a micelle-like self-assembled receptor that overcomes these limitations. The amphiphilic building block bears a moiety (i.e., Zn-metalloporphyrin) that confers specificity for a target ligand (i.e., molecules bearing basic N atoms) within the polar head. The porphyrin moiety was chosen because it allows easy monitoring of binding and assembly events using optical spectroscopy and because it makes it possible to change the nature of the target ligand by just changing the metal center. The hydrophobic body is based on a cholesterol molecule, the shape and size of which help provide the assembly with an unusually high stability. The idea is that, upon assembly of the amphiphile, Zn-porphyrin binding sites will be located within the interface water receptor, offering an easily accessible and partially desolvated environment for ligand binding, analogous in this respect to many protein binding sites.[12,18] The advantages of receptors based on the concept presented here are several: (i) the synthesis of linear amphiphilic molecules as receptors in water is likely to be simpler than that of many macrocyclic structures used so far; (ii) the assembly process brings in close proximity multiple binding sites that will increase the binding affinity of polytopic ligands through the multivalence effect;[19] and (iii) the modularity inherent in self-assembled structures allows for the easy exchange of components and offers an alternative approach to develop differential receptors.[20] Multicomponent systems often display emergent properties, i.e., properties that are not attributable to any single component but are the result of all the components working together. Understanding how these emergent properties arise is difficult, particularly when dealing with systems of high complexity, like biomolecular systems.[21] Artificial chemical systems, on the other hand, enable us to control the level of complexity. The study of such systems through the discipline of systems chemistry is leading to the exploitation of the emergent properties of multicomponent systems and also to a better understanding of biomolecular complexity.[22,23] The work presented here offers an example of a multicomponent system that is simple enough to be fully addressable but complex enough to display emergent properties: the component parts (i.e., monomers) display an enhancement of their function (recognition of the ligand) when they work within the system (i.e., after self-assembly).

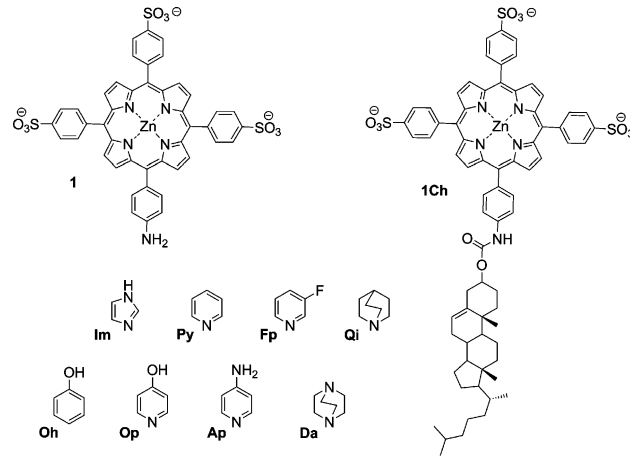

Figure 1. Chemical structure of the receptors and the ligands used in this work. **Im**, imidazole; **Py**, pyridine; **Fp**, 3-fluoropyridine; **Qi**, quinuclidine; **Oh**, phenol; **Op**, 4-hydroxypyridine; **Ap**, 4-aminopyridine; **Da**, 1,4-diazabicyclo[2.2.2]octane (DABCO).

There are few examples of the use of self-assembled discrete structures as molecular receptors in water, notably the receptors described by Fujita and co-workers.[24] Also, metallic nanoparticles have been used as scaffolds to develop molecular recognition tools.[25] However, to the best of our knowledge, receptors based on the concept presented here are not described in the literature.

Results and Discussion

Porphyrin **1** and amphiphilic porphyrin **1Ch** (Figure 1) were synthesized using standard organic chemistry procedures (see Supporting Information). Both **1** and **1Ch** are readily soluble in aqueous buffers,[26] but they show different spectroscopic properties in solution. The Soret band in the UV spectrum of **1** is sharp and follows the Beer−Lambert law in the concentration range from 0.2 to 20 μM. The structure of the band is also little affected by the addition of detergents or by using methanol as solvent instead of aqueous buffers. These results indicate that **1** is monomeric in aqueous solution and does not undergo self-association processes in the range of concentrations studied. By contrast, the Soret band of **1Ch** has a relatively low intensity and shows a broadening akin to that observed in H-type porphyrin aggregates.[27,28] Upon addition of detergent (or by

(12) Creighton T. E. *Proteins: Structures and Molecular Properties*; Freeman: New York, 1997.
(13) Moore, J. S. *Curr. Opin. Colloid Interface Sci.* **1999**, *4*, 108–116.
(14) Hunter, C. A.; Spitaleri, A.; Tomas, S. *Chem. Commun.* **2005**, 3691–3693.
(15) Israelachvili, J. N.; Mitchell, D. J.; Ninham, B. W. *J. Chem. Soc., Faraday Trans. 2* **1976**, *72*, 1525–1568.
(16) Vanhest, J. C. M.; Delnoye, D. A. P.; Baars, M.; Vangenderen, M. H. P.; Meijer, E. W. *Science* **1995**, *268*, 1592–1595.
(17) Israelachvili, J. N. *Intermolecular and Surface Forces*; Academic Press Ltd.: London, 1992.
(18) Doyle, E. L.; Hunter, C. A.; Phillips, H. C.; Webb, S. J.; Williams, N. H. *J. Am. Chem. Soc.* **2003**, *125*, 4593–4599.
(19) Mammen, M.; Choi, S. K.; Whitesides, G. M. *Angew. Chem., Int. Ed.* **1998**, *37*, 2755–2794.
(20) Anslyn, E. V. *J. Org. Chem.* **2007**, *72*, 687–699.
(21) Kitano, H. *Science* **2002**, *295*, 1662–1664.
(22) Ludlow, R. F.; Otto, S. *Chem. Soc. Rev.* **2008**, *37*, 101–108.
(23) Lehn, J. M. *Chem. Soc. Rev.* **2007**, *36*, 151–160.
(24) Tashiro, S.; Kobayashi, M.; Fujita, M. *J. Am. Chem. Soc.* **2006**, *128*, 9280–9281.
(25) Drechsler, U.; Erdogan, B.; Rotello, V. M. *Chem.—Eur. J.* **2004**, *10*, 5570–5579.
(26) Aqueous buffer refers in this works to sodium phosphate 10 mM, pH 7.2 in water, unless otherwise stated.
(27) Pasternak, R. F.; Francesc., L; Raff, D.; Spiro, E. *Inorg. Chem.* **1973**, *12*, 2606–2611.
(28) Ribo, J. M.; Crusats, J.; Farrera, J. A.; Valero, M. L. *J. Chem. Soc., Chem. Commun.* **1994**, 681–682.

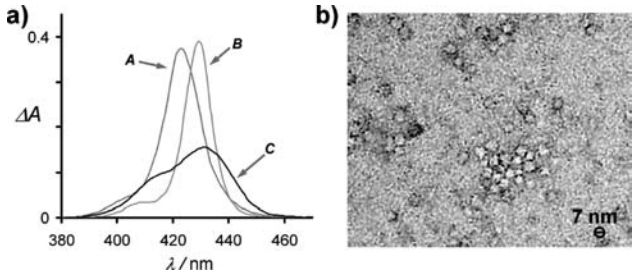

Figure 2. (a). Section of the UV absorbance spectra showing the region of the Soret band of porphyrins **1** (trace A) and **1Ch** (trace C) in aqueous buffer and **1Ch** in the presence of Triton X-100 (trace B). The concentration of **1** and **1Ch** was 1 μM in all cases. (b). Negative stain EM image of a solution of **1Ch**, 10 μM in aqueous buffer.

using methanol as solvent) the Soret band becomes sharp and intense, indicative of porphyrin de-aggregation (Figure 2a). It is perhaps not surprising that **1Ch** forms some kind of aggregate in water, owing to its amphiphilic nature, but the range of concentrations where the aggregate is detected (typical UV concentrations, i.e. between 0.5 and 50 μM) is rather low. Also, the UV spectrum follows the Beer−Lambert law, showing that the chromophore is not affected by further aggregation processes in this concentration range.

Typically, micellar aggregates have CMCs of the order of millimolar, while lower CMCs (down the micromolar to nanomolar range) are found for amphiphiles that form either membranes or cylindrical aggregates.[15−17] Interestingly, however, electron microscopy (EM) experiments reveal that **1Ch** forms virtually monodisperse spherical aggregates with a diameter of approximately 7 nm (Figure 2b). This size is consistent with a micelle-like assembly with the cholesteryl moieties pointing toward the center and the porphyrin rings on the surface (Figure 4b; see Supporting Information for molecular models). CMCs down to the milligrams per liter range (i.e., μM concentrations for amphiphiles with MW $\approx$ 1 kDa) are often determined by fluorescence using the pyrene partition method,[29,30] while determining lower CMCs requires the use of much more complex and laborious setups, including radioisotope labeling of the amphiphile.[31−33] In our case, however, **1Ch** incorporates a porphyrin moiety that is a very efficient fluorophore,[34] and this spectroscopic property can be exploited to determine the CMC of **1Ch** without the need to add an external probe. In methanol, where neither **1** nor **1Ch** forms aggregates in the micromolar range, the relative fluorescence intensity of **1** and **1Ch** at their respective maxima of excitation and emission (I_R, see Figure 3) is very similar (Figure 3a, Table 1). In water, where **1Ch** (but not **1**) forms aggregates, I_R for **1** is around 10 times larger than for **1Ch** (Figure 3b, Table 1). The low I_R of **1Ch** is attributed to self-quenching due to the close proximity of the porphyrin moieties within the aggregate.[34] These data indicate that the I_R of **1Ch** monomer in water is expected to be larger than the I_R of **1Ch** in micelles, similar to the fluorescence properties observed for **1** in water. The implication is that, when diluting **1Ch** close to the CMC, we should see an increase in the I_R as the percentage of **1Ch** monomer increases. In pure buffer the lower detection limit for **1Ch** is 10 nM. Close to this concentration there is an apparent increase of I_R, but the poor signal-to-noise ratio of the fluorescence spectrum below 10 nM prevents us from determining the CMC with any degree of accuracy. A possible solution involves raising the CMC by adding increasing amounts of methanol and then estimating the CMC in pure buffer by extrapolation.[31] The addition of methanol may also increase the I_R of our porphyrin moiety in **1Ch** (as it happens for **1**, see Table 1), lowering the detection limit of the fluorescence.[35] The addition of small percentages of methanol (between 1 and 4%) increases the I_R of **1Ch** enough to lower the detection limit down to 2 nM (Figure 3c,d; see also Figure 3SI in the Supporting Information). The plot of the fluorescence intensity against the concentration of **1Ch** in these conditions shows a sudden change in the slope of the trend line defined by the experimental data around 10 nM (Figure 3c). Addition of **1Ch** below the CMC increases the concentration of monomeric **1Ch** and the fluorescence increases linearly, with a slope that is the I_R of the monomer. Addition of **1Ch** above the CMC increases only the concentration of micelles, and the slope of the trend line is the I_R of micellar **1Ch**. Therefore, the CMC can be determined as the intersection of the trend lines defined by the pre-CMC points and the post-CMC points (Figure 3c, inset). The spectral changes associated with micelle formation can be seen by normalizing the fluorescence intensities of **1Ch** (Figure 3d). For **1Ch**, the CMC value does not increase as the percentage of methanol in the solvent increases from 1 to 4%, showing that below 4% the presence of methanol does not have a measurable impact on the CMC. This finding is in agreement with studies on the CMCs of other amphiphiles, where an exponential increase of the CMC is only clearly evident for methanol percentages above 10%.[31] Thus, the CMC value of **1Ch** in pure buffer is taken as 11 $\pm$ 2 nM, the average of all the CMC values determined between 1 and 4% methanol (see Supporting Information). Nanomolar CMCs, often found in bilayer-forming amphiphiles, have never, to the best of our knowledge, been reported for small synthetic amphiphiles (MW < 2000 Da) that form micelles.[36] A plausible explanation for the behavior of **1Ch** can be found in the unusual shape of the molecule. Amphiphiles showing low CMCs tend to have relatively large hydrophobic segments, and this normally results

Table 1. Fluorescence Excitation Spectra Parameters (Emission 612 nm)[a]

	1 (MeOH)	**1** (buffer)	**1Ch** (MeOH)	**1Ch** (buffer)
$I_{R\,max}$	1.00	0.20	0.96	0.020
λ_{max}	423	422	422	430

[a] $I_{R\,max}$ is I_R at the maximum of fluorescence intensity. λ_{max} is the wavelength of maximum fluorescence intensity in nanometers.

(29) Lee, J. Y.; Cho, E. C.; Cho, K. *J. Controlled Release* **2004**, *94*, 323–335.
(30) Wilhelm, M.; Zhao, C. L.; Wang, Y. C.; Xu, R. L.; Winnik, M. A.; Mura, J. L.; Riess, G.; Croucher, M. D. *Macromolecules* **1991**, *24*, 1033–1040.
(31) Smith, R.; Tanford, C. *J. Mol. Biol.* **1972**, *67*, 75–83.
(32) Buboltz, J. T.; Feigenson, G. W. *Langmuir* **2005**, *21*, 6296–6301.
(33) Ulrichbott, B.; Wiegandt, H. *J. Lipid Res.* **1984**, *25*, 1233–1245.
(34) Hunter, C. A.; Tomas, S. *J. Am. Chem. Soc.* **2006**, *128*, 8975–8979.
(35) Solvent polarity can affect the fluorescence quantum yield (and hence I_R) through changes in the rate of nonradiative fluorescence decay. Also, organic molecules in water tend to be especially sensitive to the presence of organic solvents due to preferential solvation. See: (a) Luo, C.; Fujitsuka, M.; Watanabe, A.; Ito, O.; Gan, L.; Huang, Y.; Huang, C. H *J. Chem. Soc., Faraday Trans.* **1998**, *94*, 527–532. (b) Narang, U.; Zhao, C. F.; Bhawalkar, J. D.; Bright, F. V.; Prasad, P. N. *J. Phys. Chem.* **1996**, *100*, 4521–4525. (c) Silva, M. A. D.; da Silva, D. C.; Machado, V. G.; Longhinotti, E.; Frescura, V. L. A. *J. Phys. Chem. A* **2002**, *106*, 8820–8826.
(36) There are in the literature a few examples of micelle-forming amphiphiles based on large molecules with very low CMC. See: (a) Chen, C.; Yu, C. H.; Cheng, Y. C.; Yu, P. H. F.; Cheung, M. K *Biomaterials* **2006**, *27*, 4804–4814. (b) Tian, L.; Hammond, P. T. *Chem. Mater.* **2006**, *18*, 3976–3984.

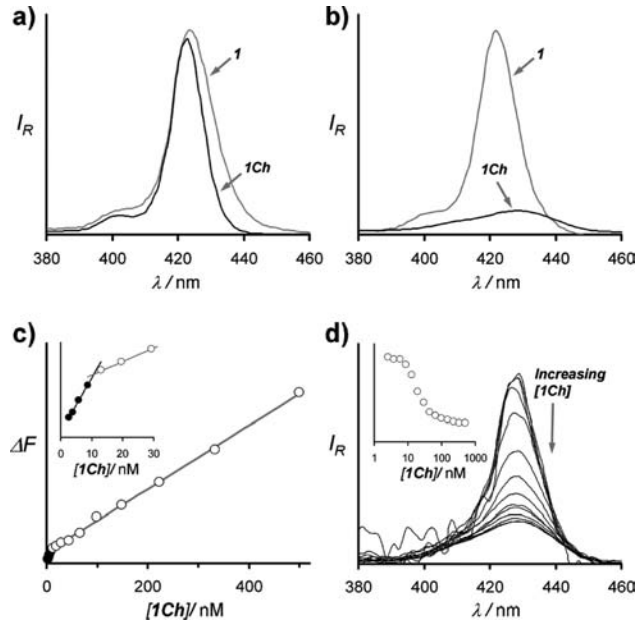

Figure 3. (a) Comparison of the relative fluorescence intensity (I_R) in the Soret band region (emission 612 nm) of **1** and **1Ch** in methanol. I_R is the fluorescence intensity corrected for the concentration of the fluorophore, e.g., $I_R = F/[\mathbf{1}]$ and $I_R = F/[\mathbf{1Ch}]$ for **1** and **1Ch** respectively. (b) Comparison of the I_R in the Soret band regions (emission 612 nm) of **1** and **1Ch** in aqueous buffer. (c) Variation of the fluorescence intensity (excitation 428 nm, emission 612 nm) with increasing concentration of **1Ch** in aqueous buffer containing 2.5% methanol. The filled circles correspond to data below the CMC, and the empty circles are for data above the CMC. The gray lines represent the best fit to a straight line. The inset shows in detail the concentration range where the change in slope is observed. (d) Changes in the I_R in the Soret band region (emission 612 nm) associated with the formation of micelles with increasing **1Ch** concentration. The inset shows the changes in I_R at 428 nm.

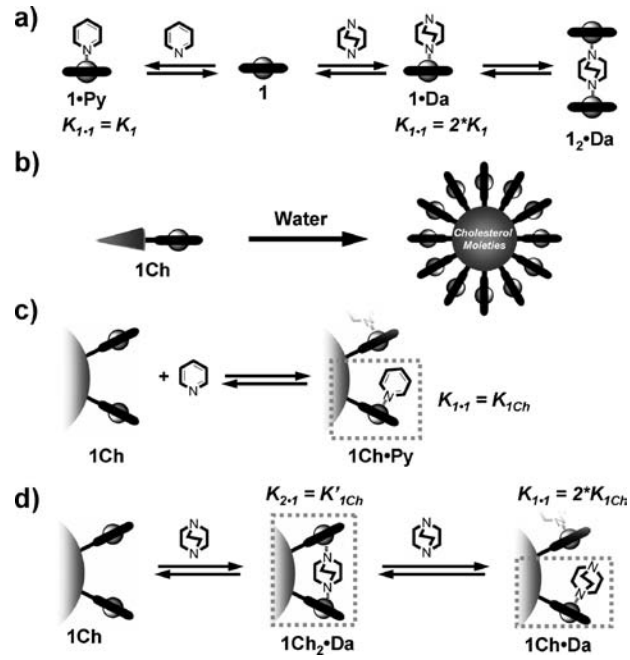

Figure 4. Cartoon representation of the formation of complexes between **1** and **Py**, **1·Py**, and between **1** and **Da**, **1·Da** and $\mathbf{1_2}$**·Da** (a); self-assembly of **1Ch** in water (b); formation of the complex between **1Ch** and **Py**, **1Ch·Py** (c); and formation of complexes between **1Ch** and **Da**, $\mathbf{1Ch_2}$**·Da** and **1Ch·Da** (d). The figure also shows the relationship between the macroscopic binding constants $K_{1\cdot1}$ and $K_{2\cdot1}$ and the statistically corrected constants K_1, K_{1Ch}, and K'_{1Ch}. For complexes with **1Ch**, the formal species that relate to the binding constants are highlighted with a dotted line frame. The complex $\mathbf{1_2}$**·Da** is shown for completeness (a) but does not form under the experimental conditions.

in a cylindrical-shaped (i.e., bilayer-forming) molecule. **1Ch**, on the other hand, has a combination of a large hydrophobic segment with a very large headgroup, resulting in a roughly conical (micelle-forming) amphiphile.[15−17] A similar example is offered by ganglioside GM1. GM1 is a lipid with a CMC of 25 nM. Pure GM1 assembles into micelles rather than into bilayers. The size of the hydrophobic segment of GM1 is responsible for the low CMC, while the unusual large size of its headgroup results in the micellar geometry of the assembly.[33] In **1Ch**'s case, the stability of the assembly could be further enhanced by the fact that the hydrophobic segment (chiefly cholesterol) is rigid.[37,38] This property may translate into a more efficient packing (and thus desolvation) upon assembly, enhancing an already favorable hydrophobic effect. In addition, the fact that cholesterol is a bulky, roughly conical molecule itself may favor the assembly into spheres as opposed to cylindrical or fiber-like assemblies, favored by flat, rigid moieties.[39−41]

Upon assembly, the Zn-porphyrin-based headgroups locate in the nanoparticle−water interface. It is well known that binding events within the interfaces of amphiphile assemblies and water are often enhanced with respect to the binding in bulk water, and this enhancement is normally attributed to desolvation, multivalence effects, or both.[18,42,43] The high stability of **1Ch** assemblies ensures that the presence of monomeric **1Ch** is negligible, allowing us to explore the desolvation and multivalence effects at the nanoparticle−water interface by simply comparing the binding parameters of **1Ch** assemblies with monomeric **1**. The binding affinities between **1** and **1Ch** and a range of nitrogen-containing ligands (Figure 1) were determined by UV titration (Table 2, Figure 5). For **1**, the statistically corrected binding constant values (K_1) are in agreement with literature data on related compounds in water.[44,45] The binding constants are also much lower (by 1−2 orders of magnitude) than for Zn-metalloporphyrin complexes in organic solvents such as chloroform,[46,47] showing the ability of water molecules to compete for the binding sites.

By contrast, **1Ch** shows a much higher affinity for the ligands than **1**, resulting in binding constants that approach values

(37) Jang, C. J.; Ryu, J. H.; Lee, J. D.; Sohn, D.; Lee, M. *Chem. Mater.* **2004**, *16*, 4226–4231.
(38) Yoo, Y. S.; Choi, J. H.; Song, J. H.; Nam-Keun, H.; Zin, W. C.; Park, S.; Chang, T. Y.; Lee, M. *J. Am. Chem. Soc.* **2004**, *126*, 6294–6300.
(39) Hoeben, F. J. M.; Jonkheijm, P.; Meijer, E. W.; Schenning, A. *Chem. Rev.* **2005**, *105*, 1491–1546.
(40) Hartgerink, J. D.; Zubarev, E. R.; Stupp, S. I. *Curr. Opin. Solid State Mater. Sci.* **2001**, *5*, 355–361.
(41) Hill, J. P.; Jin, W. S.; Kosaka, A.; Fukushima, T.; Ichihara, H.; Shimomura, T.; Ito, K.; Hashizume, T.; Ishii, N.; Aida, T. *Science* **2004**, *304*, 1481–1483.
(42) Menger, F. M.; Zhang, H. L. *J. Am. Chem. Soc.* **2006**, *128*, 1414–1415.
(43) Marchi-Artzner, V.; Gulik-Krzywicki, T.; Guedeau-Boudeville, M. A.; Gosse, C.; Sanderson, J. M.; Dedieu, J. C.; Lehn, J. M. *ChemPhysChem* **2001**, *2*, 367–376.
(44) Fiammengo, R.; Crego-Calama, M.; Timmerman, P.; Reinhoudt, D. N. *Chem.—Eur. J.* **2003**, *9*, 784–792.
(45) Mizutani, T.; Wada, K.; Kitagawa, S. *J. Am. Chem. Soc.* **1999**, *121*, 11425–11431.
(46) Taylor, P. N.; Anderson, H. L. *J. Am. Chem. Soc.* **1999**, *121*, 11538–11545.
(47) Camara-Campos, A.; Hunter, C. A.; Tomas, S. *Proc. Natl. Acad. Sci. U.S.A.* **2006**, *103*, 3034–3038.

Table 2. Binding Constants and Binding Constant Ratios (R)[a]

ligand	K_1	K_{1Ch} [R]	K'_{1Ch}
Oh	<2	<2 [nd]	
Im	63 ± 4	180 ± 18 [2.9]	
Op	15 ± 3.6	260 ± 35 [17]	
Fp	4.1 ± 0.4	175 ± 12 [43]	
Py	11 ± 1.9	340 ± 30 [31]	
Qi	520 ± 20	3100 ± 310 [6.0]	
Ap	95 ± 10	480 ± 140 [5.1][b]	3500 ± 890[b]
Da	270 ± 30	550 ± 160 [2.1][b]	14000 ± 1000[b]

[a] Binding constants are in M^{-1} units, and those for **1Ch** refer to the moles of binding sites as shown in Figure 4c,d rather than moles of assemblies; the titration experiments were performed at 303 K, and the error is quoted as the standard deviation of a minimum of three measures. For **Im**, **Py**, **Qi**, **Ap**, and **Da**, the solvent used was phosphate buffer 10 mM, pH 12.3; for **Py**, **Op**, **Oh**, and **Fp**, the solvent was phosphate buffer 10 mM, pH 7.2. At the working pH the relative amount of ligand in the free base form is ≥95% in all cases. Results for **Py** in either buffer are the same within the error. [b] Binding constants for ditopic **Da** and **Ap** were determined using a binding model that takes into account the sequential formation of 2:1 and 1:1 complexes between the **1Ch** porphyrin and the ligand. This model of binding was selected on the basis of the likely formation of the complexes depicted in Figure 4 and is consistent with the titration data (see Supporting Information). See Supporting Information for the experimental details in the determination of binding constant.

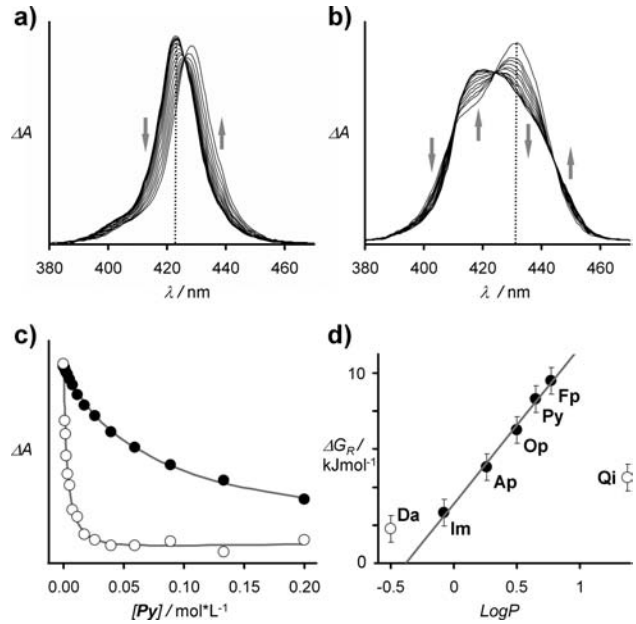

Figure 5. (a) Changes on the Soret band in the UV spectrum of **1** upon addition of **Py**. The arrows indicate the direction of change upon increasing **Py** concentration; the dotted line indicates the wavelength of the increment shown in panel c. (b) Idem for **1Ch**. (c) Changes in relative absorbance at 423 nm upon addition of **Py** to **1** (●) and at 433 nm upon addition of **Py** to **1Ch** (○). The solid lines represent the best fit to the appropriate binding isotherm (see Supporting Information). (d) Relationship between ΔG_R and the Log P of the ligands, showing the linear correlation for the aromatic ligands (●, $R^2 = 0.995$). The error bars are associated with an estimated maximum error in R of 30%.

typically found in organic solvents. Ligands that contain two basic nitrogen atoms (**Da** and **Ap**) can form complexes with two neighboring metal centers within the **1Ch** assembly, and the multivalence effect justifies in part the large value of the corresponding stability constant K'_{1Ch} (Table 2, Figure 4c).[18,34,42,43] Complexes of **1Ch** with monovalent ligands and the analogous complexes with divalent ligands (Figure 4c,d) show, however, that the increase in stability constant is a common feature for all the ligands and that this increase, expressed as the ratio $R = K_{1Ch}/K_1$, reaches values as high as 43 without the contribution of any apparent multivalence.[18] The presence of a noticeable multivalence effect for **Da** and **Ap** indicates, however, that within **1Ch** the binding sites can adopt the form of cavities defined by two porphyrin rings. Thus, for complexes defined formally as **1Ch**·L, the enhancement and modulation of the ligand binding within these interporphyrin cavities can be rationalized in terms of the combination of four factors: (i) the increase of the apparent strength of the Zn−N bond within a partially desolvated environment, due to reduced competition of water; (ii) the larger amount of hydrocarbon surface that is hidden away from water upon binding; (iii) the steric fit within these interporphyrin spaces; and (iv) the presence of an additional interaction (i.e., aromatic stacking). The quantitative assessment of each of these effects requires a very precise knowledge of the structure of the complexes and receptors that is beyond the scope of the present work. The data collected, however, allow a qualitative analysis to be made, based on the observed trends in R. There is a good linear correlation between the octanol/water partition coefficient, Log P,[48] which relates to the desolvation energy in water, and the enhancement factor R expressed in terms of free energy, $\Delta G_R = -RT \ln R$, for the aromatic ligands (Figure 5d). This correlation shows that the ligand desolvation is a major factor on binding within the assembly interface. Values for the alkyl ligands **Da** and **Qi** do not follow the same correlation as those of the aromatic ligands, suggesting that both steric fit (**Da** and **Qi** are bulkier than the aromatic ligands) and the additional interaction (i.e., aromatic stacking) may play roles in modulating the binding of the ligands. As with the aromatic ligands, it is the more hydrophobic ligand (**Qi** in this case) that displays a larger enhancement of binding (Table 2, Figure 5d). Interestingly, **Oh**, a ligand without a basic N but with a relatively large Log P of 1.5, has a very low binding affinity. This clearly shows that ligand desolvation alone is not enough to provide measurable binding within the assembly and the importance of the Zn−N bond is reinforced, due probably to the reduced competition of water within a partially desolvated environment.

Concluding Remarks

In summary, this work illustrates how the hydrophobic effect can be exploited to yield molecular receptors in the form of self-assembled nanoparticles. This result is achieved through the use of relatively small and rigid amphiphiles of unusual shape (large hydrophobic segment coupled with a very large headgroup). The nanoparticle shows an enhancement of binding for target ligands relative to a model receptor in bulk water. This enhancement is attributed mainly to two effects: (i) the reduced competition of water molecules for the binding site within the partially desolvated interface and (ii) the multivalence effect derived from the presence of multiple binding sites in close proximity. However, the different behaviors of the bulkier alkyl ligands **Qi** and **Da** suggest that also steric factors and secondary interactions (i.e., aromatic stacking) play roles in modulating the binding within the nanoparticles. The nanoparticles readily deassemble in water-miscible organic solvents such as methanol or by the addition of detergents. Receptors based on this modular concept can be easily modified by simply

(48) Experimetal values of Log P for **Im**, **Ap**, **Py**, **Fp**, **Qi**, and **Oh** were retrieved from the "Interactive PhysProp Database Demo" at http://www.syrres.com/esc/physdemo.htm. Estimated values for **Da** and **Op** were determined using Marvin/JChem 5.1 program from ChemAxon.

changing the amphiphiles of the assembly, opening the possibility for their development as differential receptors.[20] The porphyrin moiety used here as the headgroup of the amphiphiles is particularly suited for this approach; e.g. changing the metal center of the porphyrin ring is sufficient to generate a receptor with different binding selectivity. Current efforts in our laboratory aim to exploit these possibilities, which are part of the remit of the emerging discipline of systems chemistry.[22,23]

Acknowledgment. The authors thank E. F. Hounsell, K. C. Thompson, P. A. S. Lowden, H. A. J. Carless, N. H. Williams, P. Ballester, and C. A. Hunter for critical reading of the manuscript and the Faculty of Sciences at Birkbeck, University of London, for funding. EM was performed at the School of Crystallography, Birkbeck University of London, supported by a Wellcome Trust program grant to Prof. Helen Saibil.

Supporting Information Available: Experimental methods, including synthesis of **1** and **1Ch**, molecular modeling calculations, EM procedures, CMC determination experiments, and binding constant determination.This material is available free of charge via the Internet at http://pubs.acs.org.

JA900561J